Biochemical and Biophysical Research Communications 451 (2014) 436–441

Contents lists available at ScienceDirect

Biochemical and Biophysical Research Communications

journal homepage: www.elsevier.com/locate/ybbrc

Microtubule stabilization attenuates vascular calcification through the inhibition of osteogenic signaling and matrix vesicle release

Kyunghee Lee [1], Hyunsoo Kim [1], Daewon Jeong *

Department of Microbiology and Aging-associated Vascular Disease Research Center, Yeungnam University College of Medicine, Daegu 705-717, Republic of Korea

ARTICLE INFO

Article history:
Received 23 July 2014
Available online 9 August 2014

Keywords:
Vascular smooth muscle cell
Ectopic calcification
Hyperphosphatemia
Microtubule

ABSTRACT

Vascular calcification is a strong predictor of cardiovascular morbidity and mortality, especially in individuals with chronic kidney disease or diabetes. The mechanism of vascular calcification has remained unclear, however, and no effective therapy is currently available. Our study was aimed at identifying the role of dynamic remodeling of microtubule cytoskeletons in hyperphosphatemia-induced vascular calcification. Exposure of primary cultures of mouse vascular smooth muscle cells (VSMCs) to inorganic phosphate (Pi) elicited ectopic calcification that was associated with changes in tubulin dynamics, induction of osteogenic signaling, and increased release of matrix vesicles. A microtubule depolymerizing agent enhanced Pi-dependent calcification, whereas microtubule stabilization by paclitaxel suppressed calcification both in VSMC cultures and in an ex vivo culture system for the mouse aorta. The inhibition of Pi-stimulated calcification by paclitaxel was associated with down-regulation of osteogenic signal and attenuation of matrix vesicle release. Our results indicate that microtubule plays a central role in vascular calcification, and that microtubule stabilization represents a potential new approach to the treatment of this condition.

1. Introduction

Vascular calcification, which refers to the ectopic deposition of calcium phosphate crystals in the form of hydroxyapatite in cardiovascular tissue, substantially increases the risk for cardiovascular morbidity and mortality and is a common complication of chronic kidney disease, diabetes, aging, and atherosclerosis [1,2]. It is a tightly regulated and cell-mediated active process that is promoted by stimulatory factors such as inorganic phosphate (Pi), calcium, oxidative stress, osteogenic gene expression, and apoptosis as well as attenuated by inhibitory regulators such as pyrophosphate, fetuin A, and matrix Gla protein [1,3]. The mechanism underlying vascular calcification has remained unclear, however, and effective therapeutic strategies are not currently available.

Disturbance of the serum concentration of phosphate can lead to the development of hypophosphatemia (<0.8 mM) or hyperphosphatemia (>2 mM), compared with the normal concentration range of 1–1.5 mM in humans [4]. In mice, normal serum phosphate levels range from 2 to 2.6 mM, whereas animals with surgically induced chronic kidney disease manifest levels of ~3.5 mM [5,6]. The increased concentrations of Pi typically observed in hyperphosphatemic individuals promote the reprogramming and transdifferentiation of vascular smooth muscle cells (VSMCs) into osteoblast-like cells and thereby play a key role in the development of vascular calcification [3]. Vascular medial calcification associated exclusively with VSMCs has been shown to increase vascular stiffness, resulting in increased pulse wave velocity and pulse pressure and eventually leading to clinical symptoms such as hypertension and heart failure [7,8].

Modulation of cytoskeletal dynamics can itself trigger a variety of cellular signals and thereby regulate diverse cellular processes such as cell growth and differentiation [9,10]. Cytoskeletal reorganization has thus been found to regulate the activity of serum response factor as well as the expression of inducible nitric oxide synthase, the urokinase-type plasminogen activator gene, smooth muscle differentiation marker genes, and transforming growth factor-β1 [11–14].

We have now examined the possible role of dynamic changes in the microtubule cytoskeletons in Pi-induced vascular calcification. We found that microtubule stabilization by paclitaxel attenuated extracellular matrix (ECM) mineralization in VSMCs, and this effect

* Corresponding author. Address: Department of Microbiology, Yeungnam University College of Medicine, 170 Hyunchung-Ro, Nam-Gu, Daegu 705-717, Republic of Korea. Fax: +82 53 653 6628.
E-mail address: dwjeong@ynu.ac.kr (D. Jeong).
[1] These authors contributed equally.

http://dx.doi.org/10.1016/j.bbrc.2014.08.007
0006-291X/

was examined in the context of osteogenic signaling and matrix vesicle release.

2. Materials and methods

2.1. Cell and aorta organ culture

Primary VSMCs were isolated from the aorta of 6-week-old male C57BL/6J mice (Central Lab Animals, Seoul, Korea) by the explant method as described previously [15]. In brief, the isolated aorta was cut into small pieces, which were then incubated under a humidified atmosphere of 5% CO_2 at 37 °C in DMEM (Hyclone) supplemented with 20% fetal bovine serum (FBS, Hyclone) and antibiotics. At confluence, the cells were isolated by exposure to trypsin, and they were subsequently maintained in DMEM supplemented with 10% FBS and antibiotics and used for experiments between passages 4 and 6. For ex vivo organ culture, the entire mouse aorta was removed and cultured in DMEM supplemented with 10% FBS and antibiotics. Nocodazole and paclitaxel were purchased from Invitrogen. Animal experiments were approved by the Institutional Review Board of Yeungnam University College of Medicine and were in accordance with the Care and Use of Laboratory Animals.

2.2. Induction and quantification of calcification in vitro and ex vivo

To induce ectopic calcification in vitro, we exposed confluent VSMCs to calcification medium (DMEM supplemented with 10% FBS plus an additional 3 mM Pi in the form of NaH_2PO_4, pH 7.4) for 8 days or the indicated times. Calcium deposition in the cultures was visualized by staining with alizarin red S. The cells were thus fixed with 70% ethanol, and stained with 2% alizarin red S (pH 4.2). For calcium quantification, the deposited calcium was extracted with 0.6 M HCl and then analyzed colorimetrically with the use of a QuantiChrome Calcium Assay Kit (BioAssay Systems). For induction of calcification ex vivo, the entire aorta was incubated with calcification medium for 14 days. The aorta was then subjected to von Kossa staining for detection of calcium. The tissue was thus fixed with 3.7% formaldehyde and incubated in 5% silver nitrate. For quantification of aortic calcium, aortas were dried at 60 °C for 24 h, weighed, and cut into small pieces, from which calcium was extracted by incubation with 0.6 M HCl.

2.3. Assays of actin and tubulin in VSMCs

The relative amounts of F-actin and globular actin (G-actin) were determined using an F-actin/G-actin in vivo assay kit (Cytoskeleton). Cells were homogenized in F-actin stabilization buffer, after which F-actin was separated by centrifugation at 100,000*g* for 1 h at 37 °C. The resulting pellet was suspended in F-actin depolymerization buffer. For analysis of tubulin dynamics, the ratio of polymerized to free tubulin was determined using a microtubule/tubulin in vivo assay kit (Cytoskeleton). VSMCs were homogenized in microtubule stabilization buffer, and the homogenate was centrifuged at 100,000*g* for 30 min at 37 °C. The pellet containing polymerized tubulin was suspended in 200 μM $CaCl_2$. The polymerized and free tubulin fractions were then subjected to immunoblot analysis. The polymerized/free tubulin ratio was determined with the use of densitometric analysis software (Image-Pro Plus version 6.0, Media Cybernetics).

2.4. Fluorescence microscopic detection of the actin and microtubule cytoskeletons

VSMCs grown to confluency on coverslips were fixed with 3.7% formaldehyde in PBS, permeabilized with 0.1% Triton X-100. For detection of the actin cytoskeleton, the cells were incubated with fluorescein isothiocyanate (FITC)-labeled phalloidin (Sigma). For immunostaining of microtubules, cells were incubated with antibodies to β-tubulin (Santa Cruz Biotechnology) and then with tetramethylrhodamine-5-(and-6)-isothiocyanate (TRITC)-labeled secondary antibodies (Santa Cruz Biotechnology). Images of mounted slides were obtained with a TCS SP2 SE confocal microscope (Leica).

2.5. Quantitative RT-PCR and immunoblot analyses

Total RNA was extracted from cell cultures with the use of the TRIzol reagent (Invitrogen). Portions of the RNA (2 μg) were then subjected to reverse transcription (RT) followed by real-time polymerase chain reaction (PCR) analysis as performed with the use of SYBR Premix Ex Taq (Takara Bio) as well as an Applied Biosystems 7500 Sequence Detection System. Relative changes in gene expression were determined by the comparative threshold cycle method with glyceraldehyde-3-phosphate dehydrogenase (GAPDH) mRNA. Primers for PCR were synthesized by Bionics (Seoul, Korea) and are listed in Supplementary Table 1. For immunoblot analysis, cells were lysed in a solution containing 20 mM Tris–HCl (pH 7.5), 150 mM NaCl, 1% Nonidet P-40, 0.5% sodium deoxycholate, 1 mM EDTA, 0.1% SDS, and protease inhibitors (Complete tablets, Roche Molecular Biochemicals). Total cell lysates were then fractionated by SDS–polyacrylamide gel electrophoresis, and the separated proteins were transferred to a nitrocellulose membrane and exposed to primary antibodies including those to Runx2 (Cell Signaling Technology), or those to Fra-1, to SM22α, to α-smooth muscle (α-SM) actin, or to β-actin (Santa Cruz Biotechnology). Immune complexes were detected with horseradish peroxidase-conjugated secondary antibodies and ECL reagents (Abfrontier).

2.6. Isolation and characterization of matrix vesicles

For isolation of matrix vesicles, VSMC cultures were digested for 3 h at 37 °C with crude collagenase type IA (Sigma) and then centrifuged at 600*g* for 15 min, at 20,000*g* for 20 min, and at 100,000*g* for 1 h. The content of released matrix vesicles of the resultant pellet was evaluated by measurement of matrix vesicle protein content normalized by total cellular protein. A collagen calcification assay was performed as described previously [16] but with some modifications. Matrix vesicles were incubated for 72 h at 37 °C with calcification medium in culture dishes coated with collagen type I (Sigma). The deposited calcium was extracted using 0.6 M HCl and quantitated as described above. The activity of alkaline phosphatase in matrix vesicles was determined by the addition of a lysis buffer (10 mM Tris–HCl [pH 7.5], 0.1% Triton X-100, and 0.5 mM $MgCl_2$) and measurement of absorbance at 405 nm during incubation with the substrate *p*-nitrophenyl phosphate (Sigma). For analysis of calcium ion uptake, the matrix vesicles were incubated with synthetic cartilage lymph at 37 °C for 24 h, after which the vesicles were suspended in 0.6 M HCl and their calcium content was then analyzed as described above.

2.7. Statistical analysis

Quantitative data are presented as means ± SD from at least three independent experiments and were compared among three or more groups by analysis of variance (ANOVA) as performed with the SPSS 18.0 software package. When significant differences were found, pairwise comparisons were performed with the two-tailed Student's *t* test. A *P* value of <0.05 was considered statistically significant.

3. Results

3.1. Continuous exposure to Pi is essential for VSMC calcification

To study the effect of Pi on vascular calcification, we exposed mouse VSMCs to Pi at concentrations (1.5–4 mM) equivalent to those of hyperphosphatemia. Calcium quantification and alizarin red staining revealed that exposure of the cells to Pi for 8 days induced calcification in a concentration-dependent manner (Fig. 1A). Deposited calcium was first detected after treatment with 3 mM Pi for 4 days and was increased further at 8 days (Fig. 1B), indicating that the induction of VSMC calcification by Pi is also time dependent. A Pi concentration of 3 mM was selected for induction of VSMC calcification in subsequent experiments. Exposure of VSMCs to 3 mM Pi for 2, 4, 6, or 8 days followed by incubation in control medium for up to a total of 8 days revealed that the amount of deposited calcium increased in proportion to the duration of Pi treatment (Fig. 1C), suggesting that Pi is required continuously for progression of VSMC calcification. Expression of two representative VSMC lineage markers, SM22α and α-SM actin, was down-regulated in Pi-treated VSMCs, whereas that of osteoblast-specific genes, including those for bone morphogenetic protein 2, Runx2, osterix, and osteocalcin, was up-regulated (Supplementary Fig. 1). These results thus indicated that Pi triggers a phenotypic transition of VSMCs to osteoblast-like cells via osteogenic gene induction.

3.2. Cytoskeletal changes during VSMC calcification

Rearrangement of the cytoskeleton plays a key role in the contractility, proliferation, and differentiation of VSMCs [17]. To investigate the possible relation between vascular calcification and cytoskeletal reorganization, we examined the dynamics of actin and tubulin in VSMCs exposed to Pi by using fluorescence microscopic analysis as well as in vivo cytoskeletal assembly assays. The ratio of F-actin to G-actin in VSMCs was slightly, but not significantly, reduced after Pi treatment (Fig. 2A). The ratio of polymerized to free tubulin in VSMCs was increased after Pi treatment for 2 days but was markedly reduced at 4 and 8 days (Fig. 2B), coincident with the progression of calcification. These data thus indicated that microtubules are initially stabilized and subsequently disrupted during VSMC calcification, with no significant changes in actin cytoskeleton.

3.3. Modulation of microtubule cytoskeleton affects vascular calcification

Various stimuli including mechanical stress induce reorganization of the cytoskeleton in VSMCs [18], and such cytoskeletal reorganization is thought to regulate cell signaling pathways as well as cell growth and differentiation [10]. To determine whether changes in tubulin dynamics might affect vascular calcification, we cultured VSMCs in the presence of nocodazole, an inhibitor of tubulin polymerization, or paclitaxel, a microtubule stabilizer. As shown in Fig. 3A and B, treatment of VSMCs with nocodazole in the presence of Pi reduced the ratios of polymerized to free tubulin. In contrast, treatment with paclitaxel in the presence of Pi increased the ratios of polymerized to free tubulin. Induction of VSMC calcification by Pi was enhanced by nocodazole, whereas it was inhibited by the microtubule-stabilizing agent paclitaxel (Fig. 3C and D). We also obtained similar results with serum-deprived VSMCs (Supplementary Fig. 2) as well as with the mouse aorta ex vivo (Fig. 3E and F). Overall, these findings showed that microtubule disruption promotes Pi-induced VSMC calcification, whereas microtubule stabilization suppresses vascular calcification.

3.4. Paclitaxel attenuates vascular calcification via regulation of osteogenic signaling and matrix vesicle release

To characterize further the attenuation of Pi-induced VSMC calcification by paclitaxel, we examined the possible effects of this agent on osteogenic signaling. The up-regulation of osteogenic marker (Runx2, osterix, and Fra-1) expression induced by Pi in VSMCs was prevented by paclitaxel treatment (Fig. 4A and B), showing that the suppression of calcification associated with microtubule stabilization is accompanied by inhibition of osteogenic signaling. In addition, calcification in VSMCs is thought to be initiated by the release of matrix vesicles [19]. We thus found that Pi treatment increased the release of such vesicles in cultured VSMCs, and paclitaxel inhibited Pi-induced vesicle release (Fig. 4C).

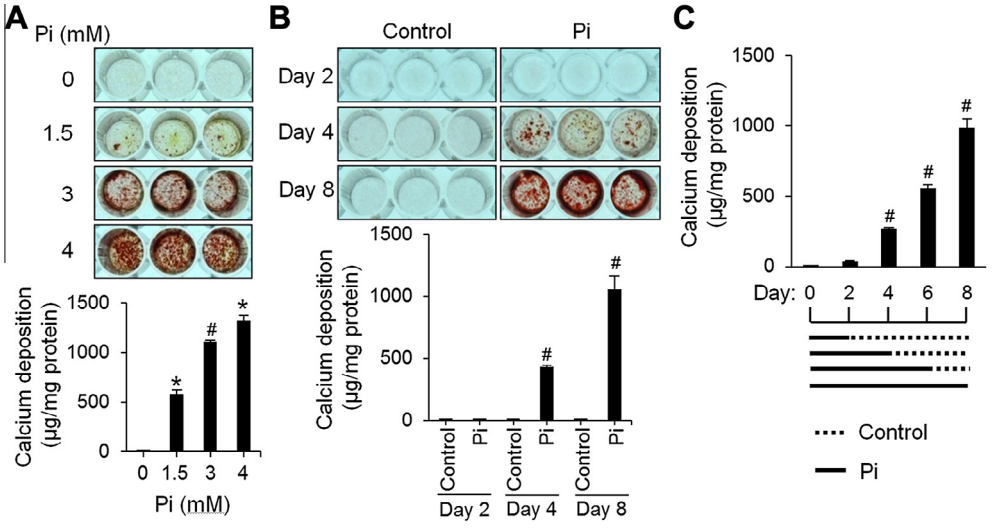

Fig. 1. Concentration- and time-dependent induction of VSMC calcification by Pi. (A) Primary mouse VSMCs were seeded in a 48-well plate (2×10^4 cells per well) and cultured for 8 days in control medium (DMEM supplemented with 10% FBS) or medium supplemented with the indicated concentrations of Pi. Calcium deposition was then visualized by alizarin red S staining, and the calcium content of the cells was quantified and normalized by protein content. Photographs of triplicate stained wells from a representative experiment are shown. (B) VSMCs were cultured in control medium or calcification medium supplemented with 3 mM Pi for 2, 4, or 8 days, after which deposited calcium was visualized and quantified as in (A). (C) VSMCs were treated with 3 mM Pi for 2, 4, 6, or 8 days and then cultured in control medium for an additional 6, 4, 2, or 0 days, respectively, after which the cells were subjected to calcium quantification. All quantitative data are means ± SD from three independent experiments. $^{*}P < 0.05$, $^{\#}P < 0.005$ versus corresponding control.

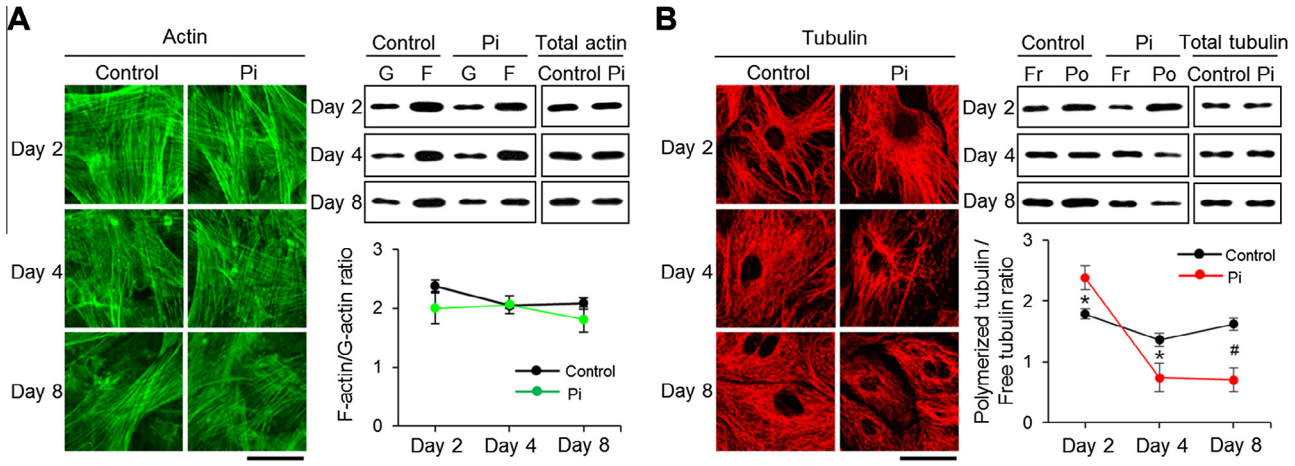

Fig. 2. Reorganization of the actin and microtubule cytoskeletons in VSMCs treated with Pi. (A) VSMCs were cultured in control medium or in calcification medium containing 3 mM Pi for the indicated times, after which the cells were either fixed for examination of the actin cytoskeleton by staining with FITC-phalloidin (left panel) or analyzed for the ratio of F-actin to G-actin (right panels). The F-actin (F) and G-actin (G) fractions were subjected to immunoblot analysis with antibodies to actin (upper right panel) followed by densitometric analysis (lower right panel). (B) Cells exposed to Pi as in (A) were either subjected to immunofluorescence staining with antibodies to tubulin (left panel) or analyzed for the ratio of polymerized to free tubulin (right panels). The polymerized (Po) and free (Fr) fractions of tubulin were subjected to immunoblot analysis with antibodies to tubulin (upper right panel) followed by densitometric analysis (lower right panel). All microscopic images are representative of three independent experiments; scale bars, 50 μm. All densitometric data are means ± SD from three independent experiments. $^{*}P < 0.05$, $^{\#}P < 0.005$ versus corresponding control.

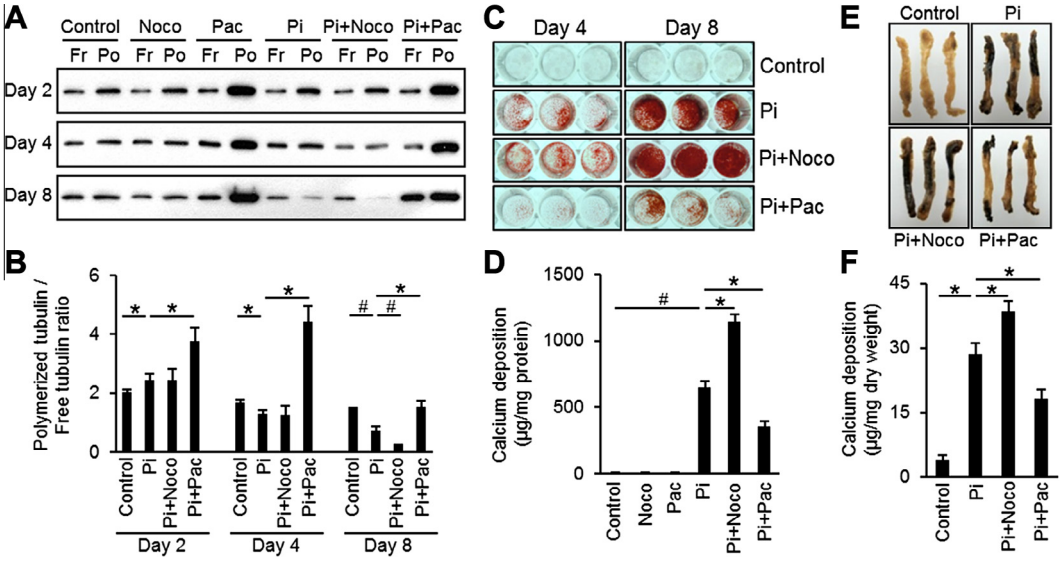

Fig. 3. Effects of cytoskeletal modulation on Pi-induced vascular calcification. (A–B) VSMCs were cultured for the indicated times with or without Pi and in the absence or presence of nocodazole (Noco) or paclitaxel (Pac), each at a concentration of 50 nM, after which tubulin polymerization status was assessed as in Fig. 2B. The polymerized (Po) and free (Fr) fractions of tubulin were subjected to immunoblot analysis with antibodies to tubulin (A) followed by densitometric analysis (B). Quantitative results are means ± SD from three independent experiments. $^{*}P < 0.05$, $^{\#}P < 0.005$. (C–D) Calcium deposition in VSMCs cultured for 8 days with or without Pi and in the absence or presence of cytoskeleton-targeted agents. Cells were stained with alizarin red S (C). The calcium content of the cells was quantified and normalized by protein content (D). Data are means ± SD from three independent experiments. $^{*}P < 0.05$, $^{\#}P < 0.005$. (E–F) Mouse aortas cultured for 14 days with or without Pi and in the absence or presence of cytoskeleton-targeted agents were subjected to von Kossa staining (E) and calcium quantification (F). Quantitative data are means ± SD from three independent experiments. $^{*}P < 0.05$.

We further found that the matrix vesicles released from Pi-treated VSMCs showed increased calcium deposition activity in a collagen matrix, increased alkaline phosphatase activity, and increased Ca^{2+} uptake compared with those released from control cells, whereas paclitaxel had no effect on these parameters (Fig. 4D–F). These results indicated that the inhibitory effect of paclitaxel on Pi-induced calcification is due to attenuation of matrix vesicle release rather than to a change in the biochemical activities of the released vesicles. Together, our findings thus suggested that stabilization of microtubules attenuates Pi-induced VSMC calcification via the inhibition of osteogenic signaling and matrix vesicle release.

4. Discussion

Hyperphosphatemia is highly associated with vascular calcification [2,4]. Increased extracellular levels of Pi have previously been shown to induce transdifferentiation of VSMCs located in the arterial media layer into osteoblast-like cells [3]. Ectopic VSMC calcification is an active cell-mediated process [1] that shares similar features with physiological bone ossification and can be divided into three distinct stages [20]. In the early stage, proliferating cells exit the cell cycle and up-regulate both collagen synthesis and alkaline phosphatase activity; the middle stage is characterized

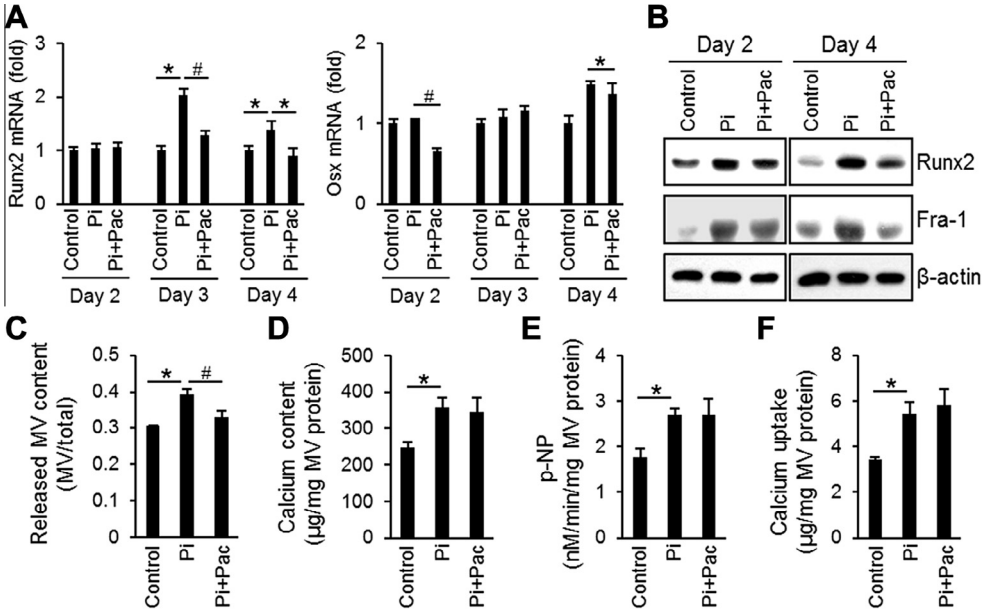

Fig. 4. Paclitaxel suppresses osteogenic signaling and matrix vesicle release during VSMC calcification. (A) Quantitative RT-PCR analysis of Runx2 and osterix (Osx) mRNAs in VSMCs cultured in control or calcification medium with or without paclitaxel (Pac, 50 nM) for the indicated times. Data were normalized by the amount of GAPDH mRNA, are presented as fold change relative to control, and are means ± SD from three independent experiments. $^{*}P < 0.05$, $^{\#}P < 0.005$. (B) Immunoblot analysis of Runx2 and Fra-1 proteins in total lysates prepared from VSMCs that had been cultured as in (A). Data are representative of three independent experiments. (C) VSMCs were incubated for 8 days with or without Pi and in the absence or presence of paclitaxel (Pac, 50 nM). The release of matrix vesicles (MVs) from the cells was evaluated by measurement of MV protein content normalized by total cellular protein. Data are means ± SD from three independent experiments. $^{*}P < 0.05$, $^{\#}P < 0.005$. (D–F) MVs released from VSMCs cultured as in C were assayed for collagen calcification activity (D), alkaline phosphatase (ALP) activity (E), and Ca^{2+} uptake activity (F). All data were normalized by MV protein content and are means ± SD from three independent experiments. $^{*}P < 0.05$.

by ECM maturation and formation of mineralization-competent matrix vesicles; and matrix vesicle release and hydroxyapatite mineral deposition occur in the late stage. We have now shown that microtubule cytoskeletons undergo dynamic changes during Pi-induced VSMC calcification. Specifically, microtubule stabilization was apparent after exposure of VSMCs to Pi for 2 days, corresponding to the early stage of calcification. Similar cytoskeletal changes were also observed at 3 h after the onset of Pi treatment (Supplementary Fig. 3) and Pi directly increased the rate of tubulin polymerization in vitro (Supplementary Fig. 4). These indicate that the microtubule stabilization apparent in the early stage of VSMC calcification is due in part to direct interaction between Pi and tubulin, and subsequent disruption of microtubule in the middle and late stages is not related to the direct effect of Pi itself.

Microtubules are essential for the execution of cell division, changes in cell shape, as well as the transport of vesicles and other organelles, and they exhibit dynamic instability [21]. Paclitaxel is a microtubule stabilizer and antineoplastic agent, having proven effective for the treatment of ovarian, breast, colon, and lung cancers [22,23]. Peak plasma levels of paclitaxel during treatment of human cancer range from 200 nM to 4 μM [24]. Myelosuppression, the main toxicity of paclitaxel, has been found to develop when plasma concentrations of the drug are maintained above an apparent threshold of 50–100 nM for >5 h [25]. The concentration of paclitaxel used in the present study (50 nM) is thus substantially lower than clinically relevant levels (0.1–10 μM) for cancer treatment [26]. In addition, paclitaxel treatment for 14 days at concentrations up to 100 nM did not have a cytotoxic effect in ureteral smooth muscle cells in vitro [27]. The potential efficacy of paclitaxel for the treatment of hyperphosphatemia-induced vascular calcification thus warrants further investigation in animal models and possibly eventually in human clinical trials.

Matrix vesicles are small membrane-bound structures that contribute to the initiation of mineral nucleation by calcifying cells [19]. We found that the release of matrix vesicles from Pi-treated VSMCs was increased compared with that from control cells. Furthermore, matrix vesicles released from Pi-treated VSMCs showed increased alkaline phosphatase, Ca^{2+} uptake, and collagen calcification activities. Although paclitaxel had no direct effect on these biochemical activities of matrix vesicles, it inhibited matrix vesicle release from Pi-treated VSMCs, suggesting that microtubule stabilization attenuates such release. In conclusion, our results suggest that hyperphosphatemia-induced vascular calcification is mediated by disturbance of microtubule dynamics and osteogenic induction. Microtubule disruption promoted Pi-induced vascular calcification, whereas microtubule stabilization inhibited such calcification by attenuating osteogenic signaling and matrix vesicle release. Our findings thus shed light on the complex process of hyperphosphatemia-induced vascular calcification, and they may provide a basis for the development of new therapeutic strategies to prevent this condition.

Acknowledgments

This work was supported by a Grant (No. A120596) from the Korea Healthcare Technology R&D Project, Ministry for Health, Welfare, and Family Affairs, Republic of Korea, as well as by grants (nos. 2013R1A1A2A10006677 and 2013R1A1A2057481) from the National Research Foundation of Korea, Korea.

Appendix A. Supplementary data

Supplementary data associated with this article can be found, in the online version, at http://dx.doi.org/10.1016/j.bbrc.2014.08.007.

References

[1] M.R. Davies, K.A. Hruska, Pathophysiological mechanisms of vascular calcification in end-stage renal disease, Kidney Int. 60 (2001) 472–479.
[2] G.M. London, Cardiovascular calcifications in uremic patients: clinical impact on cardiovascular function, J. Am. Soc. Nephrol. 14 (2003) S305–S309.

[3] S.A. Steitz, M.Y. Speer, G. Curinga, H.Y. Yang, P. Haynes, R. Aebersold, T. Schinke, G. Karsenty, C.M. Giachelli, Smooth muscle cell phenotypic transition associated with calcification: upregulation of Cbfa1 and downregulation of smooth muscle lineage markers, Circ. Res. 89 (2001) 1147–1154.
[4] X. Li, H.Y. Yang, C.M. Giachelli, Role of the sodium-dependent phosphate cotransporter, Pit-1, in vascular smooth muscle cell calcification, Circ. Res. 98 (2006) 905–912.
[5] A.P. Sage, J. Lu, Y. Tintut, L.L. Demer, Hyperphosphatemia-induced nanocrystals upregulate the expression of bone morphogenetic protein-2 and osteopontin genes in mouse smooth muscle cells in vitro, Kidney Int. 79 (2011) 414–422.
[6] S. Mathew, K.S. Tustison, T. Sugatani, L.R. Chaudhary, L. Rifas, K.A. Hruska, The mechanism of phosphorus as a cardiovascular risk factor in CKD, J. Am. Soc. Nephrol. 19 (2008) 1092–1105.
[7] J. Blacher, A.P. Guerin, B. Pannier, S.J. Marchais, G.M. London, Arterial calcifications, arterial stiffness, and cardiovascular risk in end-stage renal disease, Hypertension 38 (2001) 938–942.
[8] A.P. Guerin, J. Blacher, B. Pannier, S.J. Marchais, M.E. Safar, G.M. London, Impact of aortic stiffness attenuation on survival of patients in end-stage renal failure, Circulation 103 (2001) 987–992.
[9] C. Rosette, M. Karin, Cytoskeletal control of gene expression: depolymerization of microtubules activates NF-kappa B, J. Cell Biol. 128 (1995) 1111–1119.
[10] C. Jamora, E. Fuchs, Intercellular adhesion, signalling and the cytoskeleton, Nat. Cell Biol. 4 (2002) E101–E108.
[11] Y. Hattori, K. Kasai, Disruption of the actin cytoskeleton up-regulates iNOS expression in vascular smooth muscle cells, J. Cardiovasc. Pharmacol. 43 (2004) 209–213.
[12] A. Sotiropoulos, D. Gineitis, J. Copeland, R. Treisman, Signal-regulated activation of serum response factor is mediated by changes in actin dynamics, Cell 98 (1999) 159–169.
[13] J.P. Irigoyen, D. Besser, Y. Nagamine, Cytoskeleton reorganization induces the urokinase-type plasminogen activator gene via the Ras/extracellular signal-regulated kinase (ERK) signaling pathway, J. Biol. Chem. 272 (1997) 1904–1909.
[14] C.P. Mack, A.V. Somlyo, M. Hautmann, A.P. Somlyo, G.K. Owens, Smooth muscle differentiation marker gene expression is regulated by RhoA-mediated actin polymerization, J. Biol. Chem. 276 (2001) 341–347.
[15] H. Kim, H.J. Kim, K. Lee, J.M. Kim, H.S. Kim, J.R. Kim, C.M. Ha, Y.K. Choi, S.J. Lee, J.Y. Kim, R.A. Harris, D. Jeong, I.K. Lee, Alpha-Lipoic acid attenuates vascular calcification via reversal of mitochondrial function and restoration of Gas6/Axl/Akt survival pathway, J. Cell Mol. Med. 16 (2012) 273–286.
[16] N.X. Chen, K.D. O'Neill, X. Chen, S.M. Moe, Annexin-mediated matrix vesicle calcification in vascular smooth muscle cells, J. Bone Miner. Res. 23 (2008) 1798–1805.
[17] S.J. Gunst, W. Zhang, Actin cytoskeletal dynamics in smooth muscle: a new paradigm for the regulation of smooth muscle contraction, Am. J. Physiol. Cell Physiol. 295 (2008) C576–C587.
[18] L. Deng, N.J. Fairbank, B. Fabry, P.G. Smith, G.N. Maksym, Localized mechanical stress induces time-dependent actin cytoskeletal remodeling and stiffening in cultured airway smooth muscle cells, Am. J. Physiol. Cell Physiol. 287 (2004) C440–C448.
[19] J.L. Reynolds, A.J. Joannides, J.N. Skepper, R. McNair, L.J. Schurgers, D. Proudfoot, W. Jahnen-Dechent, P.L. Weissberg, C.M. Shanahan, Human vascular smooth muscle cells undergo vesicle-mediated calcification in response to changes in extracellular calcium and phosphate concentrations: a potential mechanism for accelerated vascular calcification in ESRD, J. Am. Soc. Nephrol. 15 (2004) 2857–2867.
[20] G.R. Beck Jr., Inorganic phosphate as a signaling molecule in osteoblast differentiation, J. Cell. Biochem. 90 (2003) 234–243.
[21] O.C. Rodriguez, A.W. Schaefer, C.A. Mandato, P. Forscher, W.M. Bement, C.M. Waterman-Storer, Conserved microtubule–actin interactions in cell movement and morphogenesis, Nat. Cell Biol. 5 (2003) 599–609.
[22] S. Haldar, J. Chintapalli, C.M. Croce, Taxol induces bcl-2 phosphorylation and death of prostate cancer cells, Cancer Res. 56 (1996) 1253–1255.
[23] A.I. Einzig, P.H. Wiernik, J. Sasloff, C.D. Runowicz, G.L. Goldberg, Phase II study and long-term follow-up of patients treated with taxol for advanced ovarian adenocarcinoma, J. Clin. Oncol. 10 (1992) 1748–1753.
[24] E.K. Rowinsky, M. Wright, B. Monsarrat, G.J. Lesser, R.C. Donehower, Taxol: pharmacology, metabolism and clinical implications, Cancer Surv. 17 (1993) 283–304.
[25] M.T. Huizing, A.C. Keung, H. Rosing, V. van der Kuij, W.W. ten Bokkel, I.M. Huinink, A.C. Mandjes, H.M. Dubbelman, H.M. Pinedo, J.H. Beijnen, Pharmacokinetics of paclitaxel and metabolites in a randomized comparative study in platinum-pretreated ovarian cancer patients, J. Clin. Oncol. 11 (1993) 2127–2135.
[26] M.E. Stearns, M. Wang, Taxol blocks processes essential for prostate tumor cell (PC-3 ML) invasion and metastases, Cancer Res. 52 (1992) 3776–3781.
[27] T.A. Will, A.J. Polcari, J.G. Garcia, M.K. Ouwenga, B.B. Voelzke, H.P. Greisler, T.M. Turk, Paclitaxel inhibits ureteral smooth muscle cell proliferation and collagen production in the absence of cell toxicity, J. Urol. 185 (2011) 335–340.